Journal of the European Ceramic Society 16 (1996) 721–737
© 1996 Elsevier Science Limited
Printed in Great Britain. All rights reserved
0955-2219/96/$15.00

0955-2219(95)00186-7

Thermal Behavior of (Organosilicon) Polymer-Derived Ceramics. V: Main Facts and Trends

M. Monthioux & O. Delverdier

Centre d'Elaboration des Matériaux et d'Etudes Structurales, UPR A8011 CNRS, BP 4347, F31055 Toulouse Cedex, France

(Received 24 April 1995; revised version received 5 October 1995; accepted 12 October 1995)

Abstract

Extensive investigations of polymer-based ceramic materials taken within the Si–C–N–O–(H) system have been performed and previously published as Parts I – IV. This paper reports the main results, facts, trends and conclusions which can be drawn from them, regarding the physical and chemical behavior of these materials submitted to an increasing thermal treatment. Both similarities and discrepancies are described and explained, whatever the chemical composition of the ceramic, (i.e. containing Si–C or Si–C–N, Si–C–O, Si–C–N–O). Emphasis is made on the mechanisms, and the role of various parameters, either intrinsic (e.g. the role of compositional C, O, or N) or extrinsic (e.g. influence of the atmosphere), is examined. The overall results indicate, among others, that excess carbon (relative to the SiC stoichiometry) is always beneficial both to the structural stability of the ceramic and the mechanical properties (when measurable), while heteroatoms (O, N) are always finally detrimental. They thus sustain the current efforts to develop ceramic fibers from chemical systems as simple as possible, using oxygen-free curing processes. More generally, they provide guidelines for understanding, and somewhat predicting, the thermochemical behavior of any related materials.

A partir d'études approfondies de matériaux céramiques issus de polymères et appartenant au système Si–C–N–O–(H), dont les résultats ont été publiés au préalable (Parties I – IV), les principaux évènements chimiques et physiques intervenant durant un traitement thermique croissant sont rappelés. Les similitudes comme les différences sont décrites et expliquées, quelle que soit la composition des céramiques (c'est-à-dire contenant uniquement Si–C, ou Si–C–O, Si–C–N, Si–C–O–N–O). L'accent est mis sur les mécanismes, et le rôle des paramètres intrinsèques (par exemple présence des éléments O, N, ou C) ou extrinsèques (par exemple influence de l'atmosphère) est examiné. D' une manière générale, les résultats indiquent, entre autres, que du carbone en excès (par rapport à la stoechiométrie de SiC) est toujours bénéfique à la fois à la stabilité structurale du matériau et à sa tenue mécanique (quand celle-ci est mesurable), alors que la présence d'hétéroatomes (O, N) est toujours préjudiciable en finale. Ces résultats vont dans le sens des efforts actuellement consentis pour développer des fibres céramiques appartenant à des systèmes chimiques aussi simples que possible, en utilisant des procédés de réticulation exempts d'oxygène. Plus généralement, ils fournissent des données de base pour comprendre, et éventuellement prédire, le comportement thermochimique de tout matériau céramique apparenté aux matériaux étudiés.

1 Introduction

Extensive studies have been performed in the past — and still are — by several French laboratories on the polymer-derived ceramics within the Si–C–N–O–(H) system. The number of papers published from these studies is huge and covers the whole field of science involved in materials preparation, so that all of them cannot be cited herein. However, a sample of related literature is proposed.[1–20] The overall goal of this governmental funded program (see Acknowledgements section) was to investigate various Si-based polymer routes and their ability to provide ceramics with high thermal stability, either for fiber or matrix purposes. Indeed, although still the best ceramic fiber commercially available nowadays, the polycarbosilane (PCS)-based NL-200 Nicalon^R fiber (Si–C–O system) is not able to respond to the needs of the 21st century (engines for aerospace or aeronautics for instance). On the other hand, polymer-based ceramic matrices (Si–C system for instance) always contain a free carbon phase, the role and behavior of which are still controversial. Thus, ceramics prepared from PCS and oxygen-cured PCS were considered as a reference series, as far as the NL-200 Nicalon^R fiber is known around the world to people involved in ceramic reinforcements for composites.

The part of the work our laboratory devoted itself to was to investigate the way the mineralized polymers (i.e. become amorphous ceramics) transform into crystallized ceramics then withstand, evolve, and degrade when submitted to an increasing thermal treatment. Because revealing the nucleation and the relative agencement of the phases was of an utmost importance, transmission electron microscopy (TEM) was used as the main investigation technique. The TEM observations, together with data from additionnal techniques such as elemental analysis, thermogravimetry, X-ray diffraction and electrical properties, all of them performed by our co-authors, were mainly reported in previous papers about ceramics from the Si–C and Si–C–O systems (Part I),[19] from the Si–C–N system (Parts II and III),[12,13] and from the Si–C–N–O system (Part IV).[20] Considering the results — in addition to some unpublished data — with some hindsight allows general trends to be revealed which are likely to help in the understanding of the thermochemical behavior of any related materials.

2 Materials

Preparation of the polymeric precursors were performed either by the Laboratoire de Chimie Organique et Organométallique (Bordeaux, France) or the Institut de Chimie Fine (Montpellier, France). The chemical aspects of the preparation have been thoroughly studied and already published or patented,[1–4,9] as has the organic/mineral transition.[7,8,10,15] Precursors for Si–C and Si–C–O ceramics were polycarbosilane (PCS) polymers, either modified from a commercial Mark 1 (ideally $[\text{–CH}_3\text{HSi—CH}_2\text{–}])^2$ or a new polymer ($[\text{–CH}_3\text{PhSi–}]_{0.5}[\text{–CH}_3\text{HSi–CH}_2\text{–SiHCH}_3\text{–}]_{0.5}$ copolymer).[1] Precursors for Si–C–N and Si–C–N–O ceramics were new polyvinylsilazane[9] ($[\text{–HSi(CH=CH}_2\text{)NH–}]$) polymer (PVSZ) or polycarbosilazane ($[\text{–CH}_3\text{CH}_3\text{Si–}]_{1-x}[\text{–CH}_3\text{HSi–N–SiHCH}_3\text{–}]_x$) copolymers (PCSZ),[3,4] where a changing x value allowed various chemical compositions to be obtained. Si–C–O and Si–C–N–O ceramics were fibers, prepared from the related oxygen-free precursors (PCS or PCSZ) by melt-spinning then curing in a nitrogen/oxygen mixture atmosphere at the Laboratoire des Composites Thermostructuraux (Bordeaux, France).[11,14,16,17] Thermal mineralisation of the polymers and further heat-treatment of the ceramic products were mainly performed by the Laboratoire des Composites Thermostructuraux for the PCS- and PCSZ-derived materials[10,11,14–18] and by the Laboratoire des Céramiques Nouvelles (Limoges, France) for the PVSZ-derived materials.[7] The mineralisation was considered to be achieved when the weight loss had become negligible, which occurred in the 800–1000°C range. At this stage, the bulk chemical compositions (obtained from Electron Probe MicroAnalysis) of the starting materials for the TEM study are (Table 1):

- $SiC_{1.4}O_{0.05}$ for the so-called Si–C ceramic (from commercial PCS);
- $SiC_{2.1}O_{0.2}$ for the so-called C-enriched Si–C ceramic (from PCS copolymer). Oxygen content originates from contamination. It mainly appears as local concentration of superficial silica and therefore does not interfere with the intrinsic evolution of the bulk ceramic. This is ascertained by the comparison between another oxygen-contaminated Si–C ceramic[9,10] and the

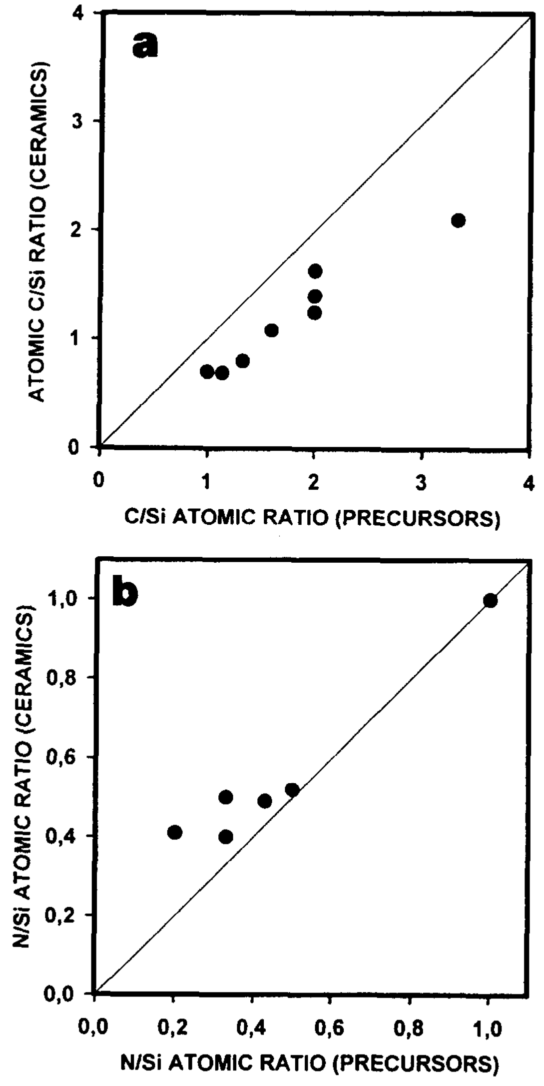

Fig. 1. Correlation between the theoretical chemical composition of the precursors and the chemical composition of the ceramic materials derived from them. (a) C/Si atomic ratio; dots below the solid line (slope = 1) indicate a depletion in C relative to the precursor. (b) N/Si atomic ratio, dots above the solid line (slope = l) indicate a depletion in Si relative to the precursor.

Table 1. Correspondence between the empirical formulae of the precursors and the elemental composition of the ceramic materials derived from them

Precursor		*Related ceramic*	
Name in the text	*Formula*	*Formula*	*Name in the text*
PCS	SiC_2H_6	$SiC_{1\cdot4}O_{0\cdot05}$	Si–C ceramic
PCS	id. (oxygen-cured)	$SiC_{1\cdot25}O_{0\cdot54}$	Si–C–O ceramic
PCS Copolymer	$SiC_{3\cdot33}H_{6\cdot33}$	$SiC_2O_{0\cdot2}$	C-rich Si–C ceramic
PVSZ	$SiC_2N\ H_5$	$SiC_{1\cdot63}N\ O_{0\cdot07}$	PVSZ-based Si–C–N ceramic
PCSZ x=0·25	$SiC_{1\cdot6}N_{0\cdot2}\ H_{5\cdot2}$	$SiC_{1\cdot08}\ N_{0\cdot41}\ O_{0\cdot05}$	
x=0·75	$SiC_{1\cdot14}\ N_{0\cdot43}\ H_{4\cdot28}$	$SiC_{0\cdot69}\ N_{0\cdot49}\ O_{0\cdot05}$	PCSZ-based Si–C–N ceramic
x=1	$SiC\ N_{0\cdot05}\ H_4$	$SiC_{0\cdot7}\ N_{0\cdot41}\ O_{0\cdot06}$	
x=0·5	$SiC_{1\cdot33}\ N_{0\cdot33}\ H_{4\cdot66}$	$SiC_{0\cdot8}\ N_{0\cdot5}\ O_{0\cdot05}$	
PCSZ x=0·5	id. (oxygen-cured)	$Si\ C_{0\cdot8}\ N_{0\cdot41}\ O_{0\cdot6}$	Si–C–N–O ceramic

same but contamination-free ceramic,[19] the thermal behaviour of which are similar;

- $SiC_{0\cdot8}N_{0\cdot5}O_{0\cdot05}$ for the so-called Si–C–N ceramic (from PCSZ copolymer, for $x = 0\cdot5$);
- $SiC_{1\cdot25}O_{0\cdot54}$ for the so-called Si–C–O ceramic (from commercial PCS)
- $SiC_{0\cdot8}N_{0\cdot4}O_{0\cdot6}$ for the so-called Si–C–N–O ceramic (from PCSZ copolymer, for $x = 0\cdot5$).

Whatever the chemical system the ceramic samples belong to (Si–C, Si–C–N, Si–C–O, Si–C–N–O), differences in their chemical composition at the end of the mineralisation stage are somewhat well-related to the basic differences in the chemical composition of the precursors, specifically regarding the carbon content (see Table 1 and Fig. 1). The fact that the C/Si atomic ratios are always lower in the ceramics than in the precursors (Fig. 1(a)) has to be related to the weight loss occurring during the organic/inorganic transition episode which is mainly due to the removal of gaseous hydrocarbon species. However, the fact that the N/Si atomic ratios are higher or equal in the ceramics compared to the precursors (Fig. 1(b)) may indicate that Si-containing species are also removed during the mineralisation stage.

Thermal stability of the above ceramics was then investigated through further heat treatments under a high purity argon flow (N56 grade) up to 1600°C or more using a 3600°C/h heating rate and a 0·25 or 1 h isothermal stage (graphite crucible in a radio frequency coil). Weight losses with increasing temperature were most often measured in a graphite crucible and furnace in N56 grade argon flow (SETARAM TAG 24). Some other treatments may have been using specific conditions and will be mentioned in the text. Attention has to be paid that, as far as possible, treatment conditions were standardized for all the samples above. Conditions were different for the Si–C–N ceramic prepared from the PVSZ polymer (lower heating rate, nitrogen atmosphere,...). Comparison with the ceramics above is then not allowed, except in some cases. Therefore, the chemical composition (from chemical analysis) of the related starting material is now given for information ($SiC_{1\cdot63}NO_{0\cdot07}$) but cannot be compared to the compositions above without caution. Results on PVSZ-based ceramics will be only used in Sections 3.3.4, 3.4.4, 3.5.2, and 3.5.3.

TEM investigations were performed using high resolution microscopes from PHILIPS (EM400 and CM12). Conventional bright field (BF), lattice fringes (LF) and selected area diffraction (SAD) modes were used, in addition to a peculiar dark field mode (DF) the principle of which is detailed in refs 5 and 19. Aperture sizes used provided a resolution limit of 0·65 nm in DF mode, and allowed lattice periods higher than 0·23 nm to be imaged in LF mode. Observations and previous conclusions were mainly published in references 12, 13, 19, and 20.

Further experimental details were provided in the previous papers already cited.

3 Results and Discussion

3.1 Thermal behavior of the polymer-based ceramics: common trends

All the starting materials of the study are amorphous ceramics, as evidenced from SAD patterns and DF images, exhibiting a fine (<1 nm) porosity. Regarding the chemical system they belong to, crystallyzed phases such as SiC, Si_3N_4, SiO_2, and C were expected to occur at a given time of the thermal treatment. Specifically, regarding the C/Si at. ratio values, one could expect the occurrence of a 'free' carbon phase for materials with a C/Si at. ratio higher than 1 (i.e. above the value for the SiC stoichiometry). In fact, any of the materials develops a free carbon phase, whatever the C/Si at. ratio, even for values as low as 0·70 (Si–C–N ceramic for $x = 1$). Of course, this indicates that part of the Si atoms are mobilized by the N atoms (and/or O atoms) and are therefore no longer available to make SiC. Actually, free carbon is always the first phase to nucleate, generally as so-called Basic Structural Units (BSUs) which are small stacks of 2–3 polyaromatic layers (graphenes) of 1 nm in lateral extension and piled up as plates in turbostratic order (Fig. 2). Because BSUs have also been observed in other 'immature' carbon-containing ceramic materials (such as Nicalon^R NL200 or Tyranno^R Fibers)[21,22] on the one hand, and have been demonstrated to be the primary state of solid carbon in most of the polyaromatic carbon materials[23] on the other hand, it is believed that nucleation of BSUs must be a common event for any polymer-based ceramic, as soon as excess carbon is available. According to previous studies on the Nicalon^R NL200 fiber[21] and as sustained by other investigation methods such as NMR,[24] BSUs are found to act as independent entities, and the peripheral carbon atoms of graphenes tend to be saturated with hydrogen atoms rather than to be linked to the surrounding medium. Modelling the BSUs as shown in Fig. 2 then taking into account the H content may thus be a way to estimate the free carbon content of the ceramics through simple calculations, and good concordances have been found when possible.[12,21,24] Aromatic CH groups are not stable at high temperature and, as in any carbon material,[25] hydrogen is removed mainly as gaseous H_2 in the 1000 – 1250°C range, as revealed by elemental analysis,[12] mass spectrometry,[21] or NMR.[24] This induces unsaturations which are fixed by the edge-to-edge linkage of neighboring BSUs into larger distorted graphene stacks (Fig. 3). As the thermal treatment continues to increase, the distorted graphene stacks continue to associate each other edge-to-edge and, in a lesser extent, face-to-face. They thus increasingly build a polyaromatic carbon network, which may finally be possibly interconnected at long distance depending on the amount of free carbon phase relative to the bulk. According to the scenario above, a hydrogen-depleted immature ceramic, (i.e. having not enough remaining H atoms to saturate the peripheral C atoms of the coronene-like graphenes of the BSUs, the H/C atomic ratio of which is ~ 0·5)

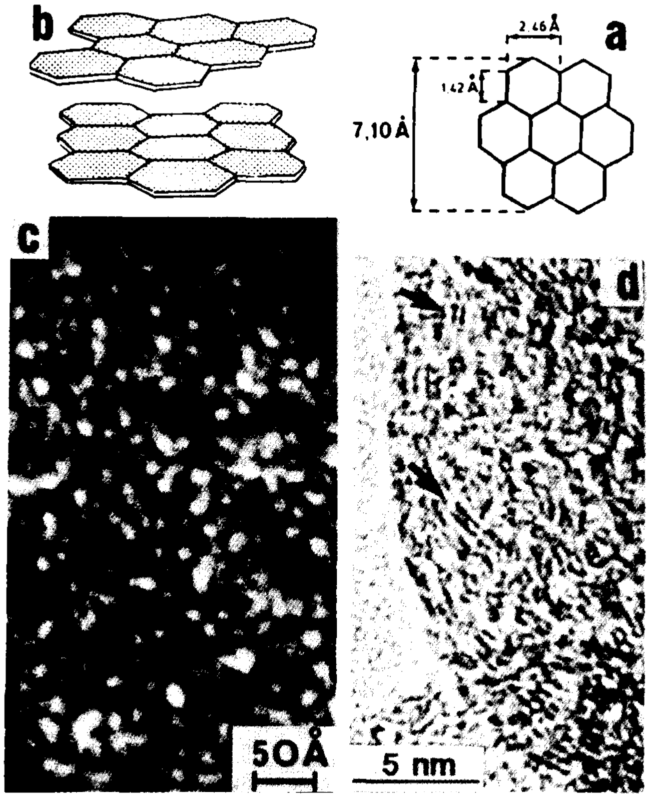

Fig. 2. (a) Sketch of a coronene molecule. (b) Sketch of a BSU. (c) Because of their tiny size, BSUs appear only as bright dots in DF mode the size of which is close to the resolution limit. (d) Imaging them in LF mode is possible (arrows) but requires drastic conditions of sample thickness and focussing values.[21]

Fig. 3. LF image of distorted graphene stacks obtained from the removal of peripheral hydrogen atoms of BSUs and subsequent BSU edge-to-edge association (example taken from a PCSZ-based Si–C–N ceramic with $x = 0·1$).

needs to make the amount of peripheral aromatic C atoms match with the amount of available H atoms, and then may have a very narrow temperature window between the occurrence of BSUs and their subsequent edge-to-edge association. The step of BSU occurrence may thus be missed.[19]

SiC is always the second phase to nucleate, as nanometric crystals, even for the N-containing ceramics, which probably has to be related to the fact that the N/Si atomic ratios of the starting ceramic materials are always lower than the value N/Si = 1·33 required for the stoichiometry of Si_3N_4. As soon as the grain sizes are large enough to provide reliable LF images, the SiC crystals appear associated to the carbon phase, in the manner that the graphenes tend to lie flat upon the crystal faces (Fig. 4). This suggests that, as far as BSUs nucleate first, they could act as nuclei for SiC, by promoting the stacking of alternate Si then C atom layers from the graphene faces. Indeed, on the one hand the BSU and SiC primary grain sizes are similar (about 1 nm), and on the other hand the lattice parameters of a graphene and of SiC are somewhat compatible (Fig. 5).[26] However, this remains a mere assumption and would require further investigations, such as looking at C-depleted ceramics, which were not available materials. Whatever, the graphene stacks / SiC grains association is an undoubted fact, which at least may originate from the structural rearrangements from BSUs to distorted layers, which naturally will tend to dispose according to the minimal free energy state, i.e. flat upon any free surface (specifically when the surface somewhat presents a lattice compatibility).

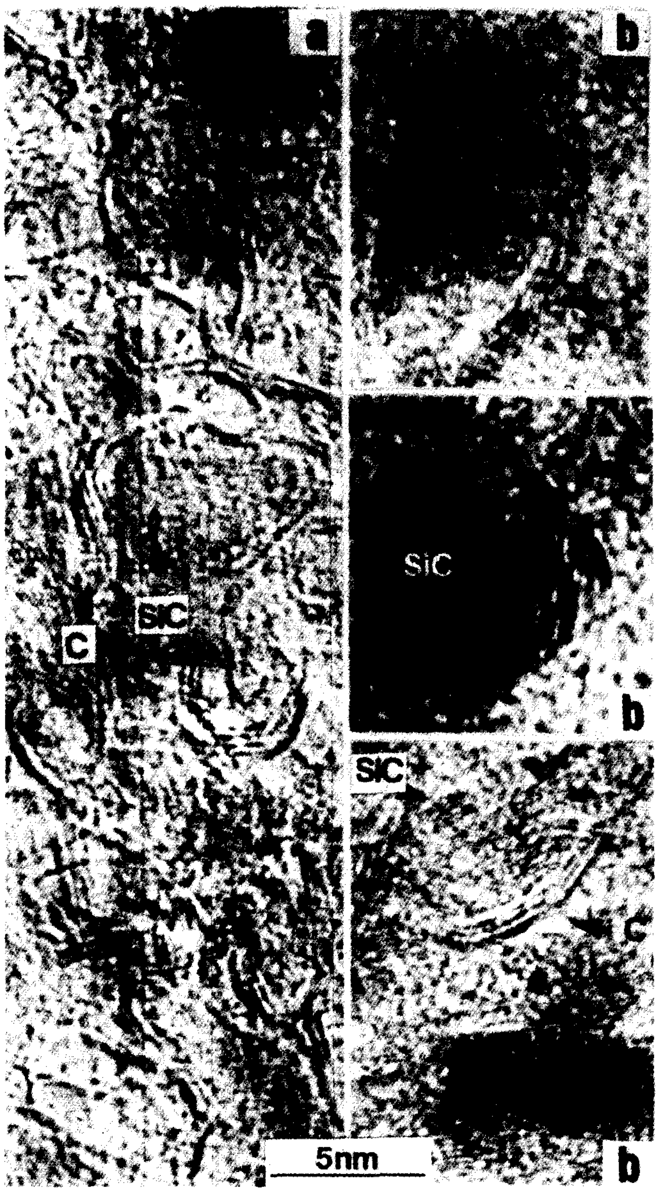

Fig. 4. LF images of distorted graphene stacks lying flat upon SiC crystal faces. (a) example taken from a Si–C ceramic (with C/Si at. = 1·4).[19] (b) Examples taken from a PCSZ-based Si–C–N ceramic with $x = 0{\cdot}5$.[13]

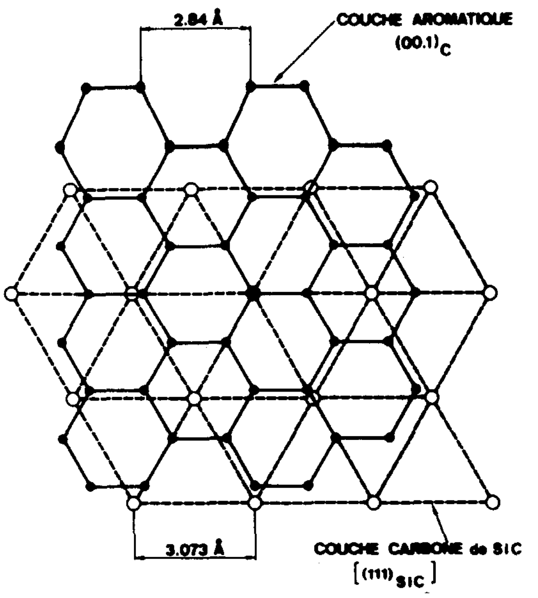

Fig. 5. Sketch of the superimposed lattices of a graphene and of a C layer in a β-SiC crystal seen following the [111] direction.[26]

At this stage of their thermal evolution, all the polymer-based ceramics investigated are made up

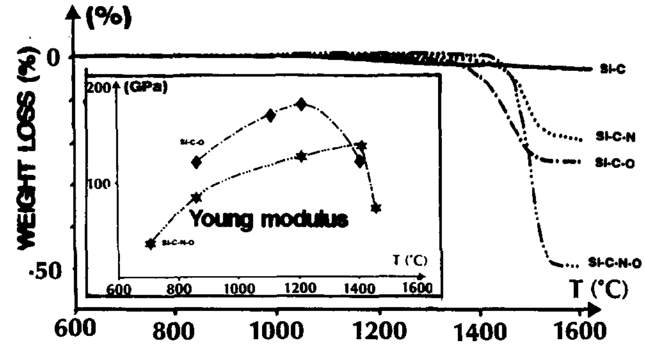

Fig. 6. Weight loss versus heat-treatment temperature for various ceramics submitted to standard conditions of heat-treatment (the Si–C–N ceramic is PCSZ-based with $x = 0{\cdot}5$). The temperature of weight loss corresponds to the temperature of degradation of the heteroatom-containing intergranular phase. Consequently, Si–C appears as the only stable system. In inset: example of mechanical property degradation for fibered ceramics, to be related to the time of the intergranular phase degradation.[11,17,19,20]

of more or less large SiC crystals (but generally less than ~ 10 nm), a more or less interconnected polyaromatic carbon network in which SiC crystals are inserted as within uncomplete carbon cages, and a more or less abundant intergranular amorphous $SiC_xO_yN_z$ phase (thus containing the heteroatoms — O, N – when any). SiC crystals are not like dry hazelnuts in their shells relative to the intergranular phase but must be linked to it, in order to account for the level of mechanical properties observed ($E \sim 200$ GPa, see inset in Fig. 6 for instance). Whether Si–C ceramics (i.e. not containing any heteroatoms) also have a real amorphous SiC_x intergranular phase or merely SiC_4 grain boundaries is a question, which cannot be ruled out by TEM. It cannot be easily answered either by spectroscopic methods such as NMR or XPS for instance, because of the coexistence of both ordered but nanometric (SiC crystals) and disordered (amorphous SiC) structures, both containing SiC_4 tetrahedra. Considering the fact that SiC grains do not appear much larger nor more frequent in Si–C ceramics than in heteroatom-containing ceramics, it is doubtful that the whole bulk of the Si–C ceramic is able to completely transform into crystalline SiC nuclei in a same time. Kinetic effects are expected, depending on how favorable to arrange into a β-SiC structure neighboring SiC_4 tetrahedra are. We thus assume that a remaining amorphous SiC_x intergranular phase is still present between SiC grains in Si–C ceramics, from which the SiC crystals will be built then will grow up, at least during the first growth step.

Actually, SiC crystals always grow up slowly in a first step then drastically in a second step, following various and multiple growth mechanisms which depend both on the temperature range and the chemical system the materials belong to (see Section 3.3). As expected from thermodynamic calculations,[27] the Si–C system is very stable and does not exhibit any weight loss, contrary to the heteroatom-containing ceramics (Fig. 6). Thus, in any system but the Si–C system, the second growth step originates in the diffusion-controlled thermochemical degradation of the heteroatom-containing intergranular phase, which in turn is able to degrade the free carbon phase through solid–solid reactions (Si–C–N ceramic)[13] or gas–solid reactions (Si–C–O and Si–C–N–O ceramics),[19,20] as illustrated in Fig. 7. Since depending on the diffusion of gaseous species through the material towards the outer surface, the degradation rate is slow enough to induce skin/core effects. The degradation starts in areas close to the outer surfaces then proceeds towards the inner parts. The coexistence of two grain growth mechanisms in a ceramic is thus possible for a while, the low rate growth in the core, and the high rate growth in the skin.[19,21] When ceramics are under a filamentous shape (oxygen-containing systems), the thickening of the skin with the increasing temperature is measurable,[14] somewhat revealing the diffusion ability of the gaseous species involved. Also, testing the mechanical behavior is possible in that case, and performances fall down drastically (inset in Fig. 6) as soon as both the intergranular phases (i.e. the amorphous and the carbon ones) degrade. As far as the second SiC crystal growth step always occurs both at high temperature and corresponds to a high rate growth, stacking faults become

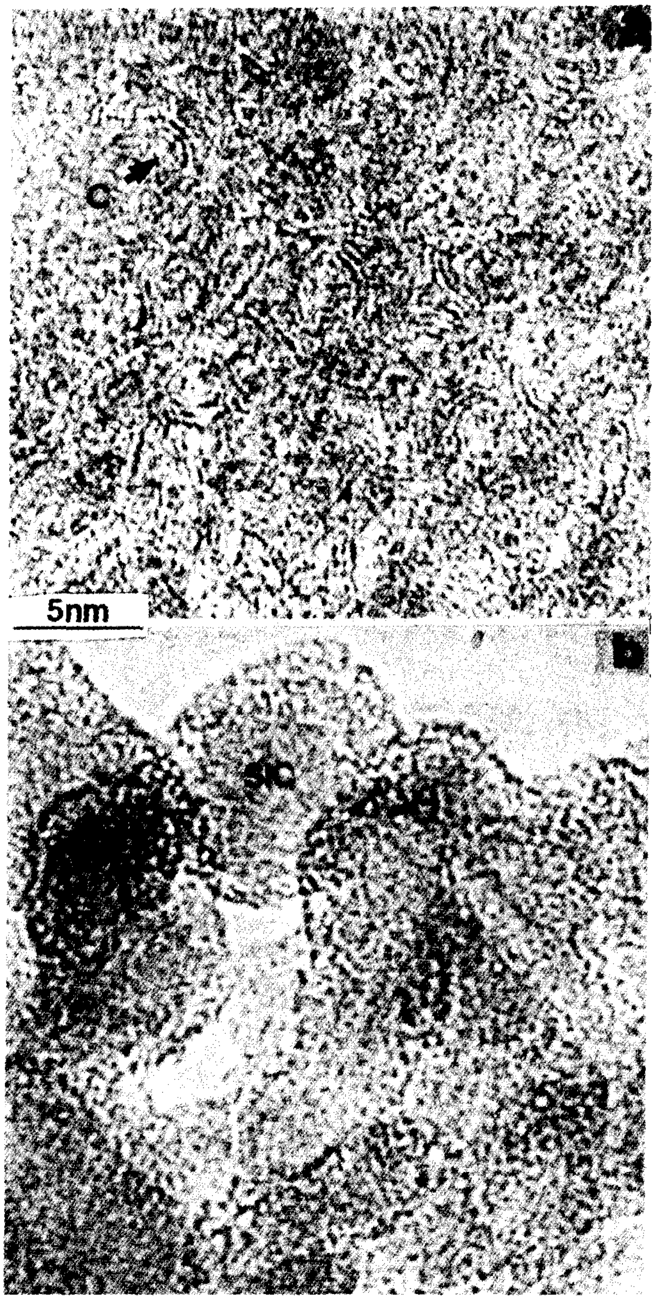

Fig. 7. LF images of Si–C–O ceramic materials in the vicinity of the degradation temperature. (a) In inner parts, where the material is not degraded yet, polyaromatic carbon stacks still are well visible (arrows). (b) In outer parts, where the thermochemical degradation has started, carbon stacks are destroyed and are no longer visible.[19]

frequent, and the mere β structure is progressively replaced by polytypes.

3.2 Chronology of events

All the chemical, structural and textural events described above are common to any of the ceramics here studied, and even to other related materials.[21,22] However, for similar heating rate, they occur at temperatures which may vary depending on the chemical system. Table 2 gathers all the data[12,13,19,20] about the temperature of occurrence for the main events which are likely to characterize the thermal evolution of polymer-based ceramics. Following the general trends above, these events are: the nucleation of BSUs ('BSU'), the edge-to-edge association of BSUs into distorted graphene layers ('d'), the nucleation of SiC crystals ('Cr'), then the thermochemical degradation of the heteroatom-containing intergranular phase ('★'). Attention has to be paid that the edge-to-edge association of the BSUs ('d' event) is related to the building of the carbon network, but does not mean whether the network is interconnected at long distance or not. The interconnection event is not reported in Table 2, since it is related to the amount of free carbon content, which cannot directly be quantified by TEM images. Table 2 only involves ceramic materials heat-treated in similar conditions (i.e. Si–C–N ceramics from PVSZ are excluded). The comparison between the various systems is believed to be as more accurate as the architectures of the starting polymers are close. Also, Si–C–N ceramics from PCSZ with x values other than 0·5 are not considered in Table 2, since they have not been investigated following enough accurate temperature steps. When between parenthesis '(BSU)' indicates that the stage of BSU nucleation was missed because of the inadequate temperature step for the final temperatures of the heat-treatments, which were sometimes not narrow enough. However, knowing that the BSU nucleation must occur after the amorphous state but before the edge-to-edge BSU association helped us to estimate the temperature of BSU nucleation in these cases. Generally speaking, the temperatures of event indicated are rigorously the temperatures at which the related events have been observed for the first time rather than the temperatures at which they have really occurred, i.e. the event may have occurred sooner, within a temperature range which has not been investigated.

As already mentioned in Section 3.1, nucleation of BSUs is then the first event to occur. Despite the tiny size of the BSUs (< 1 nm), a specific use of the TEM technique allows them to be identified and distinguished from the background.[19] Attention has to be paid that nucleation and concentration of polyaromatic carbon may pre-exist as single graphenes without being revealed by TEM, as far as our imaging procedure needs the stacking period between graphenes to occur (corresponding to the 002 reflection). However, developments of such single graphenes are very limited, since thermodynamic indicates[28] that face-to-face association of graphenes are favored as soon as the graphene size reaches that of the coronene molecule (about 0·7 nm). We thus assume that the BSU occurrence may really be considered as the starting point of the development of a 'free' carbon phase. From Table 2, it is clear that heteroatoms (O, N) unfavor the BSU nucleation. Coarsly, the temperature of BSU nucleation is as higher as the atomic C% is lower (Fig. 8), unsurprisingly due to an effect of increasing dilution which acts against the necessity for carbon atoms to be close to each other to be able to associate into graphenes then into graphene stacks. More in detail, the correlation in Fig. 8 is not very

Table 2. Chronology of the main physicochemical events characterizing the thermal evolution of some of the polymer-based ceramic materials investigated. Heat-treatment conditions were similar. BSU = BSU nucleation. d = edge-to-edge association of BSUs into distorted graphene stacks. Cr= SiC crystal nucleation ★ = thermochemical degradation of the heteroatom-containing intergranular phase. The Si–C–N ceramic reported is PCSZ-derived with x = 0·5.

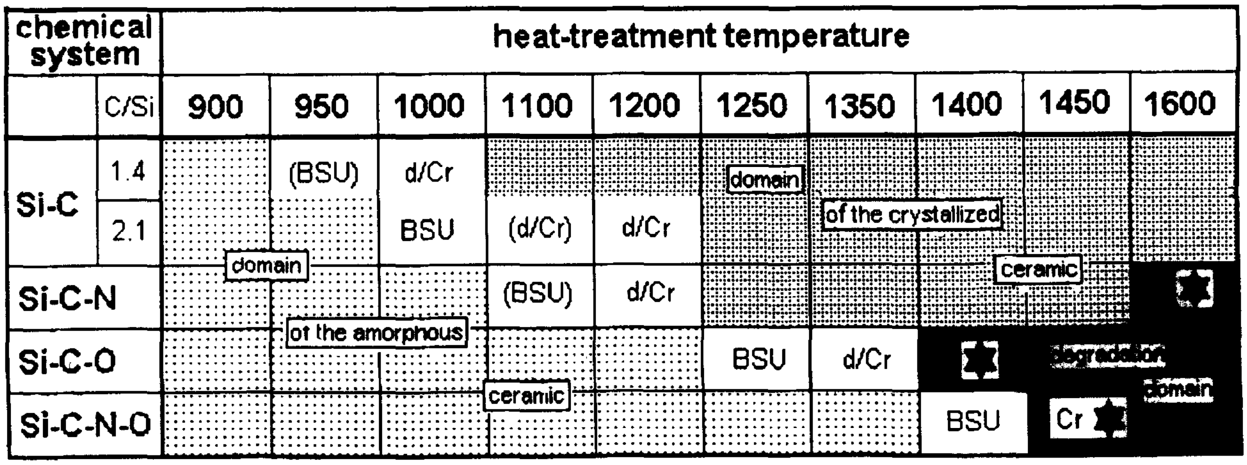

chemical system		heat-treatment temperature									
	C/Si	900	950	1000	1100	1200	1250	1350	1400	1450	1600
Si-C	1.4		(BSU)	d/Cr							
	2.1			BSU	(d/Cr)	d/Cr					
Si-C-N					(BSU)	d/Cr					★
Si-C-O							BSU	d/Cr	★		
Si-C-N-O									BSU	Cr ★	

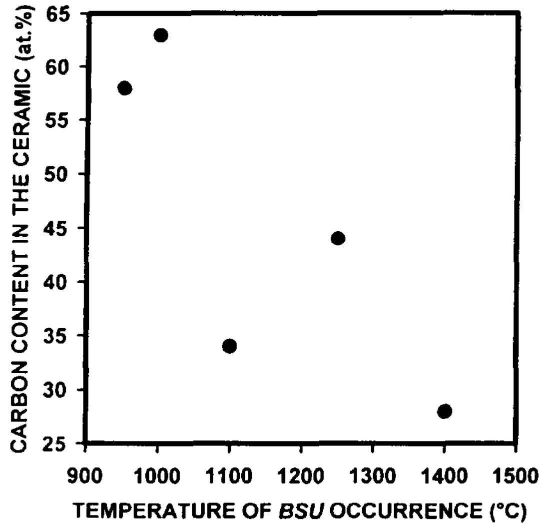

Fig. 8. Correlation between the temperature of BSU occurrence and the carbon content for the various ceramics listed in Table 2.

good, because of various and multiple reasons which would be too much speculative to discuss (differences in the polymer architecture, relative affinity of O and/or N for Si and/or C, role of the remaining H atoms,...). At least, as discussed in Section 3.1, the lack of sufficient amount of remaining H atoms in the Si–C ceramic relative to the C-enriched Si-C ceramic may have caused an early building of the carbon network, while the highest atomic C content — as in the C-enriched Si-C ceramic — would have been expected to induce the earliest BSU nucleation, statistically speaking.

As soon as BSU nucleation has occurred, the edge-to-edge association of the BSUs into distorted graphene stacks ('d' event in Table 2) follows quickly, generally related to a release of gaseous H_2. Building the carbon network is thus the second event to occur (together with the SiC nucleation), except in the Si–C–N–O ceramics. Indeed, BSUs nucleate as late as 1400°C in the latter, while the bulk material degrades within the following 50°C only. Obviously, BSUs do not have the time to associate in that case. In addition, it may be questionable whether BSUs which are that late could behave exactly the same way than earlier BSUs, specifically regarding the saturation by peripheral hydrogen atoms, as far as aromatic CH groups may not exist at this temperature.

Except for the Si–C–N–O ceramics, the nucleation of SiC crystals ('Cr' event in Table 2) then appears to be concomitant to the edge-to-edge association of BSUs. It is thought to be a coincidence, since studying the Si–C–N ceramics from PVSZ (which are not reported in Table 2 because of the discrepancies in the heat-treatment conditions) has shown that both events could be successive, the BSU association occurring first.[12] Indeed, as assumed above, the BSU association is believed to be a consequence of the removal of the hydrogen atoms peripheral to the graphenes, while the nucleation of SiC crystals has to be related to structural rearrangements at the solid state within the remaining amorphous $SiC_xN_yO_z$ matrix (where y and/or z may be equal to 0 depending on the chemical system, of course). Actually, Table 2 indicates that the nucleation of SiC is logically the earliest in the Si–C ceramics, as far as structural rearrangements towards SiC_4 tetrahedra are expected to be much easier in a SiC_x matrix than in a heteroatom-containing matrix. On the opposite, the SiC nucleation is the latest in the Si–C–N–O ceramics, i.e. containing two types of heteroatoms having no affinity one to each other but with Si atoms, which is also assumed to be the best situation to unfavor structural rearrangements towards SiC_4. Again, using TEM to evidence the nucleation of the SiC crystals is probably the most convenient technique, but induces some limitations. Primary SiC crystals are revealed both through the SAD and DF modes, based on the cristallographic reflections of pure β-SiC. Therefore, local concentrations of SiC_4 tetrahedra which would be non-ordered or ordered otherwise (as clusters for instance) would be missed, while possibly acting as the nuclei. However, the first β-SiC imaged may be as low as 1 nm large, which only corresponds to few elemental cells (about 8, containing about 30 SiC_4 tetrahedra).

Finally, the last event is, of course, the thermochemical degradation of the ceramics ('★' event in Table 2), which occurs through the thermochemical degradation of the remaining amorphous $SiC_xN_yO_z$ matrix. From Table 2 (no '★' event in Si–C ceramics) and Fig. 6, it is obvious that the threshold of thermal stability of the ceramics is governed by the presence and the type of heteroatoms, while the amount of them must be more related to the intensity of the degradation. Nitrogen (Si–C–N ceramic in Table 2) appears more likely to induce a thermally stable intergranular phase than oxygen (Si–C–O ceramic in Table 2). This has to be related to the stability of Si–N bond relative to the Si–O bond in the specific environment of the carbon-containing ceramic materials investigated, which would need thermodynamic calculations. It at least has probably to be related to the value of the N/Si atomic ratios which are always by far under the stoichiometry of Si_3N_4 (1·33), and obviously remain so even after the mobilisation of some of the Si atoms due to the crystallisation of SiC. As a matter of fact, ceramics containing both O and N (Si–C–N–O ceramic in Table 2) exhibit a degradation temperature intermediate between that of Si–C–O and Si–C–N ceramics.

3.3 Mechanisms of crystal growth

Depending on the chemical system the ceramics belong to the temperature range of the heat-treatment, and the composition of the atmosphere, various mechanisms of SiC crystal growth may occur, which are described below.

3.3.1 Annealing type

Figure 9 summarizes the evolution of the SiC grain sizes for the ceramic materials also reported in Table 2 (again, Si–C–N ceramic from PVSZ are excluded because of the discrepancies in the treatment conditions). The SiC grain size is represented by the modal size, i.e. the class of the most frequent size. Actually, SiC grain sizes never have a single value at a given temperature but a range of values with various frequencies. A complete description of the grain size evolution thus should require to draw histograms from a statistical investigation. This has been performed sometimes, in this study[19] or — mainly — in a previous one.[21,29] However, such work is very time-consuming and using the modal size, which is rather easily estimated by a mere but carreful eye-examination of the DF images, has been most often preferred. Figure 9 shows that at least two growth rates may be identified for all the ceramics, whatever the system. The first one is low and corresponds to the growth of SiC grains within the domain of thermal stability of the bulk material. It is encountered in every ceramics — but the Si–C–N–O ceramic, (see Section 3.3.2 below) — as soon as the SiC crystals have nucleated. Indeed, the SiC nucleation necessarily goes with the formation of grain boundaries (either between SiC grains or between SiC grains and the remaining amorphous phase). They concentrate internal stresses, the energy of which is higher as the mismatch between the two adjacent lattices is higher. With the

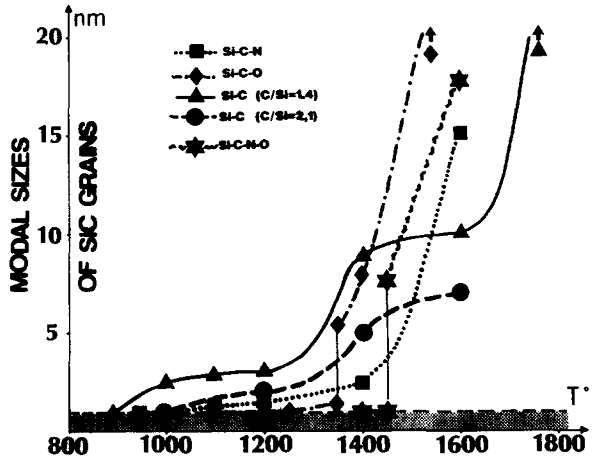

Fig. 9. Modal size of SiC crystals versus heat-treatment temperature for various ceramics submitted to standard conditions of heat-treatment.[13,19,20] Strictly speaking, the modal size is the class of the most frequent size, and therefore may be different from the mean size. Two values are given for the Si–C–O and Si–C–N–O fibered ceramics at 1350 and 1450°C respectively, since a skin/core effect occurs at these temperatures (see text). For the latter (Si–C–N–O), the grain sizes value are indicative only, since a size gradient occurs in addition to the skin/core effect.[20]

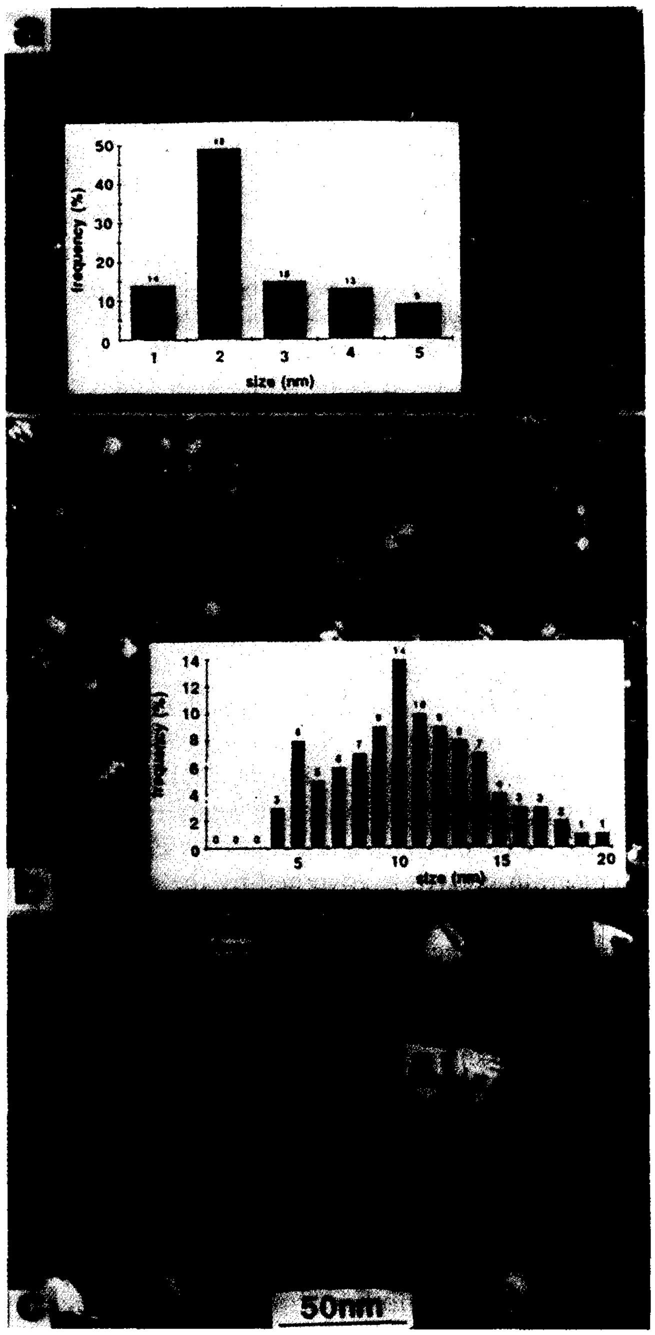

Fig. 10. Typical DF images and some related grain size distributions for various grain growth mechanisms. (a) Within the stability domain. The image is typical from a nucleation then low rate growth step following the annealing mechanism. Example taken from a Si–C ceramic (with C/Si at. = 1·4). In inset, the related grain size histogram.[28] (b) Within the degradation domain. The image is typical from a rapid grain growth through the coalescence mechanism. Example taken from a Si–C–O ceramic. In inset, the related grain size histogram.[29] (c) Peculiar case of the Si–C–N–O ceramic, in which the SiC nucleation and the $SiC_xN_yO_z$ phase degradation are concomitant.[20] Note the difference in grain shapes between (b) — round grains — and (c) — triangular grains. The image suggests a low rate growth step following an atom-by-atom feeding mechanism.

increasing temperature, stresses tend to relax and structural rearrangements occur at the grain boundaries, through the diffusion and migration of the structural defects. The crystal growth cannot occur otherwise than following random directions, since depending on only the interfacial energy which governs the defect migration, instead of following specific crystallographic directions. Crystal shapes are therefore isometric (Fig. 10(a)), and crystal sizes increase as the temperature increases. The growth rate remains low since occurring at the solid state, and at a relatively low temperature. Crystal size distributions are generally narrow and asymetric, i.e. the most frequent size classes are the lowest (Fig. 10(a)), since the memory of the nucleation event is not far and the chances of structural rearrangements are low. However, they of course increase as the temperature increases. As already pointed out in Section 3.2, at a given temperature within the low growth rate domain, crystal sizes tend to be higher in the Si–C ceramics than in the Si–C–N or Si–C–O ceramics (Fig. 9), due to the better chemical compatibility of the surrounding matrix regarding the SiC crystals, making easier the structural rearrangements.

3.3.2 Atom-by-atom feeding

In Si–C–N–O ceramics, SiC crystal nucleation is completely inhibited by the presence of O and N atoms in the bulk matrix. The nucleation can only occur when the heteroatoms are removed, i.e. when the $SiC_xN_yO_z$ phase degrades. Likewise, the subsequent grain growth is governed by the degradation rate. Since N and O do not leave the system at the same speed,[20] the material is structurally and texturally deeply transformed but the transformations may be slow enough to induce a crystal size gradient within the skin in addition to the skin/core effect mentioned in Section 3.1. Because the nucleation step and the subsequent grain growth step occur almost in the meantime and at high temperature, the stable intergranular phase cannot form, but the coalescence growth mechanism (see Section 3.3.3 below) cannot occur at this stage either. Finally, features suggest another growth type. Actually, crystals formed no longer exhibit isometric shapes but elementary crystallographic shapes such as tetrahedral, which are evidenced by triangular projections when the crystals are lying on a (111) face relative to the electron beam (Fig. 10(c)).[20] This reveals a low rate growth mechanism able to respect the respective expansion rate of the various crystal faces of the face centered cubic, thus promoting the 'slow' faces (111) to the detriment of the 'fast' faces (100) and (110). This is consistent with an atom-by-atom feeding mechanism, similar to that occurring in oversaturated solutions (when the required atoms are easily available, every crystal faces may take the number of atoms they need to grow up). The mechanism is likely to proceed as long as the 'feeding' matrix remains in an amount high enough to prevent crystal impingements. As soon as this condition is no longer fulfilled, the coalescence type growth mechanism may occur (see Section 3.3.3 below).

3.3.3 Coalescence type

The mechanism of growth by coalescence corresponds to the high growth rate domain in Fig. 9 and finally occurs in any ceramic, as supported by the slopes of the curves which are the same for all of them. It appears as soon as SiC crystals become free of any linkage to the surrounding medium. Because of the high temperatures on the one hand and of the relatively small size of crystals on the other hand, SiC crystals may be led to move and to impinge, due to thermal energy supply. Impingements lead to coalescence and subsequent high rate crystal growth. Again the growth cannot be oriented following specific crystallographic directions and the grain shape tends to be isometric (Fig. 10(b)). Since larger crystals are relatively less likely to move than smaller ones, chances of coalescence are lower for them. The subsequent grain size distributions therefore tend to provide wide and symetric histograms (inset in Fig. 10(b)). Crystals are less and less numerous, but larger and larger.

It is amazing to state that all the ceramics develop this peculiar growth mechanism, whatever the chemical system they belong to, while they do not all behave identically under thermal stress. Why SiC crystals become free to move in Si–C–N and Si–C–O ceramics is clear. As long as the remaining matrix which partly surrounds the SiC crystals as an intergranular phase and which they are linked to is stable, the grain growth is limited to the structural solid-state rearrangements mentioned in Section 3.3.1. As soon as the temperature becomes high enough to make the bonds the heteroatoms (O, N) are involved in break, the SiC crystals are liberated and may start to move, impinge, then coalesce with the neighboring crystals. For most of the materials, the intergranular carbon network cannot prevent this mechanism to occur, since generally also being degraded in the meantime. The high temperature growth mechanism is the same for the Si–C–N–O ceramics, and it is noteworthy that the grain shapes change from tetrahedric (Fig. 10(c)) to isometric as soon as the coalescence mechanism occurs.[20]

It has been assumed that an SiC_x intergranular phase may also exist in Si–C ceramics (see Section 3.1). Specifically in these materials, as long as the intergranular phase exists, SiC crystals are built from it, and the building rate may increase quickly as the temperature increases, much more quickly than in the heteroatom-containing ceramics because of the chemical compatibility between the crystals and the surrounding matrix. This explains the intermediate rapid growth episode in Fig. 9 for SiC ceramics. Afterwards, because both the possibilities of structural rearrangements are exhausted and because the intergranular carbon network partially hinders the coalescence growth mechanism, the grain growth is limited for a while. This explains the intermediate slow growth episode in Fig. 9. Finally, the grain growth may start again following the expected coalescence mechanism as soon as the energy supply and the subsequent thermal 'shaking' is high enough to make the crystals go out from the uncomplete carbon cages and finally impinge on to each other. Another reason for the SiC crystals leaving the carbon cages is that, as the temperature increases, the carbon structure improves, rigidifies, and become less and less able to accommodate the SiC grain growth. This may induce internal stresses able to finally expel the SiC grains. Anyway, from this point, the carbon phase is no longer systematically intricated with the SiC phase but tends to evolve apart.[19]

Consistently, it is doubtful that, for the very large crystals which are obtained in any ceramic at very high temperatures, the coalescence mechanism remains the main one. Sizes may have become high enough to oppose to wide movements, which would be needed. Thus, other mechanism — such as that occurring in thermally sintered materials — are expected to occur and progressively replace the previous one, but they have not been able to be revealed in the study.

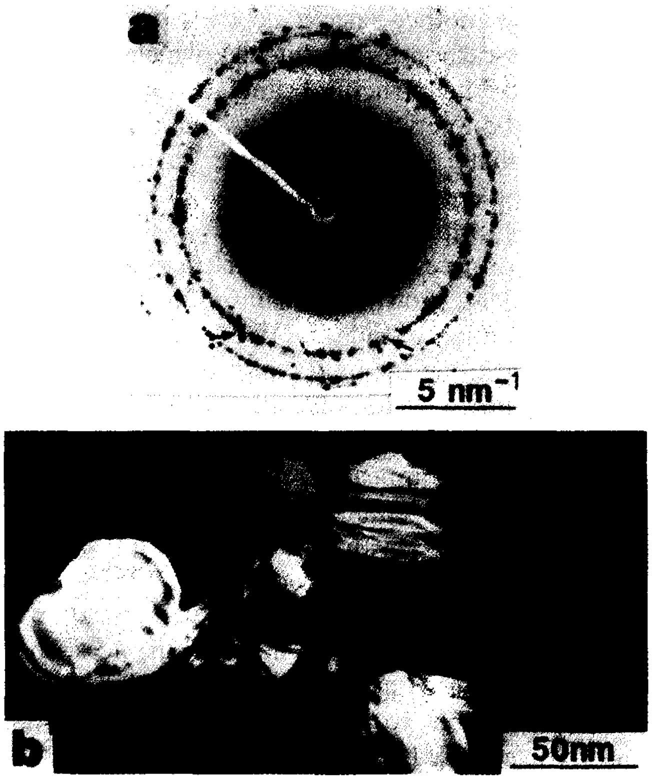

Fig. 11. Examples of evidence for polytypism in ceramic materials. (a) SAD pattern: peculiar features of polytypism are arrowed. (b) DF image: the spiral aspect (arrow) suggests a helicoidal growth mechanism, as for whiskers.

3.3.4 Vapor growth type

Because the intergranular phase degradation involves gaseous species such as N_2 (in Si–C–N ceramics), SiO and CO (in Si–C–O and probably Si–C–N–O ceramics), and possibly radicals, vapor growth mechanisms in heterogeneous (gas–solid) or homogeneous (gas–gas) phases are expected at high temperature within the high rate growth domain, according to reactions such as:

$$\mathrm{Si(g) + CO(g) \rightarrow SiC(s) + 1/2\ O_2(g)} \qquad (1)$$

$$\mathrm{SiO(g) + CO(g) \rightarrow SiC(s) + O_2(g)} \qquad (2)$$

$$\mathrm{SiO(g) + 2\ C(s) \rightarrow SiC(s) + CO(g)} \qquad (3)$$

$$\mathrm{Si(g) + C(s) \rightarrow SiC(s)} \qquad (4)$$

which are amongst the most probable.

Homogeneous reactions such as (1) and (2), specifically, are believed to be responsible for the occurrence of polytypes, always revealed in high temperature SAD patterns (Fig. 11(a)) or DF images (Fig. 11(b)). Actually, a growth mechanism such as coalescence is more likely to provide twin crystals, for instance, than the peculiar alternance of polytypes stacked and aligned following the [001] (regarding the regular α-SiC structure) or [111] (regarding the regular β-SiC structure) directions as observed in Fig. 11(b). Such structural features are rather found in rapidly grown SiC crystals such as that obtained from chemical vapor deposition process[30] or whisker preparation process,[31] which both occur following the quick propagation of a screw dislocation in conditions of undersaturation (when few atoms are available, it is more easy to promote the grain growth by only adding them at the step of a dislocation). The mechanism must be thus concomitant to the coalescence mechanism, since it requires the intergranular phase degradation to occur. However, the latter is certainly generally prevalent, at least for a while, since it is more likely to explain why grain size histograms are symmetrical (see Section 3.3.3), while a vapor growth mechanism may affect any crystal regardless its size and should much more quickly induce asymetrical histograms with a predominance of the largest size classes.

Heterogeneous reactions such as (3) and (4) are also likely to participate in SiC grain growth, to an extent which may be very variable from one ceramic to another since it depends on the ability of the free-carbon to be attacked, which is directly related to the structural and textural features of the carbon network, if any. Actually, the chemical reactivity of polyaromatic carbon mainly occurs by the edges as it is nearly nil by the faces. Therefore, graphene edges or, at least, structural defects, are necessary. Such a mechanism may be the prevalent growth mechanism in PVSZ-based Si–C–N ceramics. Indeed, PVSZ-based ceramics were found to be the only ones the SiC nucleation step was not a widespread occurrence at a given temperature everywhere in the material.[12] SiC crystals, when they appear, are randomly distributed but seldom, with grain size distributions which are not consistent with that of a regular nucleation then growth process (Fig. 12). Because of the early development of a widespread, well formed and complete carbon network (the free-carbon content is about 32 at%),[12,24] very few carbon atoms remain available to make SiC, and the SiC_xN_y matrix is enclosed in carbon cages. The formation of SiC crystals thus appear to be related to the random occurrence of available graphene edges, due to the breaking of graphene–graphene grain boundaries induced by thermally promoted internal stresses (Fig. 13).

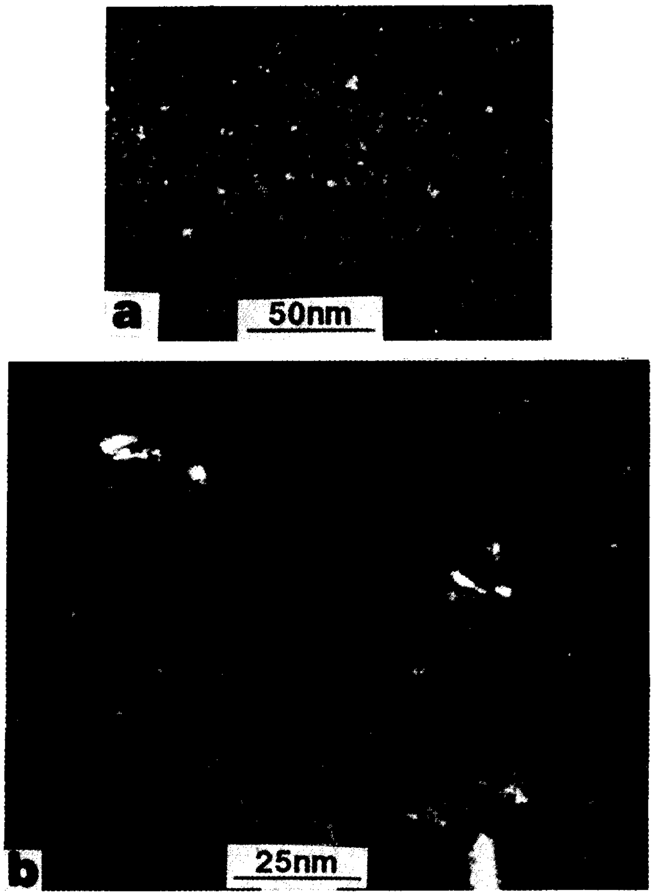

Fig. 12. DF images of the SiC crystal distribution at temperatures close to the step of SiC nucleation in (a) a PCS-based ceramic material, taken as a reference for a regular nucleation mechanism: there are many small crystals and (b) a PVSZ-based Si–C–N ceramic: the crystals are rare and large.

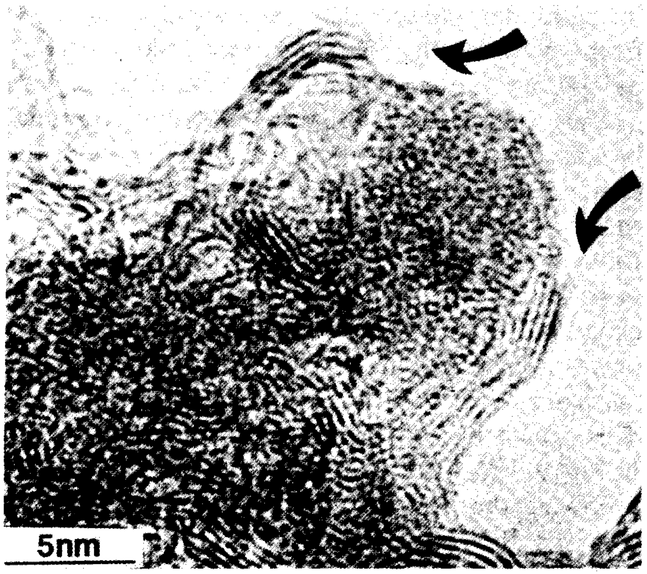

Fig. 13. LF image as an example of graphene edges become accessible due to the breaking of a carbon cage in a PVSZ-based Si–C–N ceramic.[12]

Contrarily, Si_3N_4 crystals are never formed in Si–C–N ceramics (under argon atmosphere), while the gaseous species cited in the following reactions have been directly detected[17] or are very probable:

$$3\ Si(g)+2N_2(g) \rightarrow Si_3N_4(s) \qquad (5)$$

$$3\ SiO(g) + 2N_2(g) + 3\ CO(g) \rightarrow Si_3N_4(s) + 3\ CO_2(g) \qquad (6)$$

This indicates that the required amounts of some of the related species are not available, either because they may have been preferentially used for SiC-promoting reactions (see above), or merely because quantities released were not sufficient.

3.4 Influence of intrinsic parameters (i.e. related to the polymer composition)

3.4.1 Role of the carbon content

Increasing the carbon content within the polymer always goes with increasing the free carbon content in the subsequent ceramic. A well developed carbon network is always favorable to the thermal stability of the ceramics, as far as it is detrimental to the SiC grain growth, either because opposing to the structural rearrangements as an intergranular phase, or because preventing the coalescence mechanism as uncomplete carbon cages. For instance, the comparison between the Si–C ceramic and C-enriched Si–C ceramic in Fig. 9 is clear regarding that point. Within the same simple chemical system (Si–C), SiC modal sizes are always lower for the latter than for the former at given temperatures, though the bulk behavior of growth remains identical. The carbon phase may even improve some mechanical features such as the Young modulus as soon as the carbon network interconnects at long distance.[21] As long as it is not chemically destroyed by the thermochemical degradation of heteroatom-containing intergranular phase, it is also assumed to help in maintaining the mechanical cohesion of the ceramic material within the coalescence growth domain or, at least, in providing some flexibility to the bulk material. As a matter of fact, the latter feature may be required for the weaveability of heteroatom-free (or poor) SiC fibers, such as the new Hi-Nicalon^R or Tyranno^R Lox-E which are now being studied.[32–34]

It also appears clearly that the electrical behavior of the ceramic is deeply and mainly influenced by the behavior of the carbon phase, at least for temperatures up to 1400°C (Fig. 14), beyond which the contribution of the SiC phase becomes prevalent (because of the carbon phase degradation) or no longer subordinate (when the carbon phase does not degrade). In Fig. 14, the materials are as more conductive (less and less semi-insulator) as E_a decreases.[10,11,13,17,19,20] and the slope of the curve $E_a = f(T)$ must at least partly be related to the speed the carbon network becomes long-range interconnected at. Indeed, considering the temperature of events the SiC phase is involved in (nucleation, crystal growth) does not correlate well with the electrical behavior of the various ceramics. For instance, the nucleation of SiC occurs later in the C-enriched ceramic (with C/Si at. = 2.1) relative to the Si–C ceramic (with C/Si at. = 1.4), while the resistivity decreases more rapidly for the former. On the contrary, taking (arbitrarily) the Si–C ceramic as the reference sample, it appears that the respective pathes of the various ceramics may be directly related to the carbon phase behavior. Actually, the beginning of the loss of the semi-conductor feature occurs the earliest in the C-enriched ceramic because of the quick carbon network interconnection expected from the higher free carbon content, it occurs later in the Si–C–N ceramic due to the later carbon network building, and it occurs the latest in the Si–C–N–O ceramic because no carbon network is able to build. Likewise, the fact that the behavior for the Si–C–O ceramic seems not to follow the same general path as for the other ceramics could be explained by the fact that the carbon network is probably destroyed before being long-range interconnected, making the electrical behavior mainly controlled by the non-carbon phases. Also, an insufficient amount of free-carbon may be a reason. Finally, tentatively characterizing the carbon network interconnection event by the inflexion point of the curves in Fig. 14, we could say that the interconnection occurs around 1050°C for the C-enriched Si–C ceramic, around 1100°C for the reference Si–C ceramic, and around 1200°C for the Si–C–N ceramic.

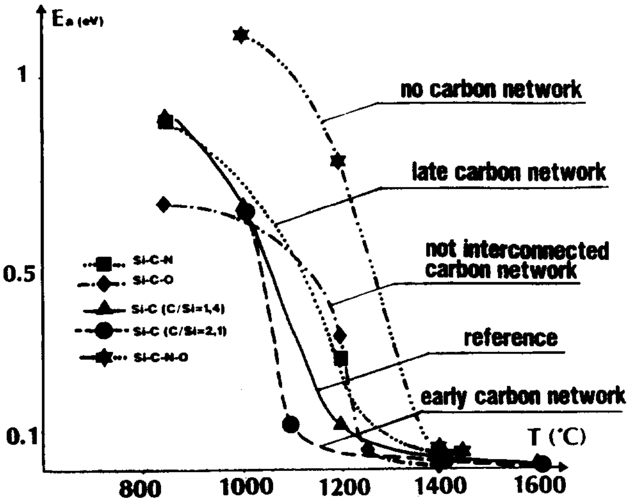

Fig. 14. Electrical behavior of some ceramic materials versus the increasing final temperature of heat-treatments (as measured T_f $\theta = 230°C$, in order to avoid any possible machine effect for insulating materials). The plot is based on the variation of the apparent activation energy E_a calculated from the slope of log10 $\sigma = f(1/\theta)$ instead of the absolute conductivity values, in order not to have to take into account shape factors, which could be unknown or unprecise for bulk materials (four-point method, measurements from room temperature to ~ 600°C, helium atmosphere).[10,11,13,17,19,20] The Si–C ceramic (with C/Si at. = 1·4) is arbitrarily taken as the reference material which the others are compared to.

3.4.2 Role of the oxygen content

Oxygen is not involved in the primary chemical composition of the polymer precursor, strictly speaking, since added during the organic/inorganic transition process as a curing step. However, it is incorporated very early and is therefore considered here as an intrinsic parameter. Using such oxygen-containing polymers allows both the nucleation of SiC (and of BSUs) and the subsequent grain growth to be delayed, through the development of an intergranular phase the oxygen atoms are concentrated in. Oxygen atoms thus hinder the structural rearrangements towards SiC. From a structural standpoint, oxygen-containing ceramics (Si–C–O, Si–C–N–O) evolve less quickly than the related oxygen-free ceramics (Si–C, Si–C–N), and therefore may be considered more structurally stable within the thermochemical stability domain. However, the oxygen-containing intergranular phase is always thermally unstable, which finally results in a deep chemical alteration of the bulk material. From this standpoint, oxygen is detrimental to ceramic materials devoted to high temperature applications.

3.4.3 Role of the nitrogen content

Of coarse, using nitrogen-containing polymers allows the same nucleation then growth inhibition effects to be obtained than with oxygen, i.e. nitrogen-free ceramics (Si–C, Si–C–O) evolve more quickly than the related nitrogen-containing ceramics

(Si–C–N, Si–C–N–O), structurally speaking. Nevertheless, as mentioned in Section 3.4.2 above, nitrogen is less efficient than oxygen regarding these inhibition effects. On the contrary, the intergranular phase the nitrogen atoms are concentrated in is thermochemically more stable than the oxygen-containing intergranular phases. From this standpoint, nitrogen is less detrimental than oxygen to ceramic materials devoted to high temperature applications. However, the role of nitrogen cannot be that simple. Because the N content appears to act both on the nucleation, the free carbon content, and the degradation of the material, increasing the N content does not lead to monotonous changes in the ceramic behavior.[13] For instance, a high N content unfavors the nucleation then growth of the SiC phase, and also unfavors the development of the C phase by delaying the BSU nucleation and enhancing the carbon network degradation. Both events are antagonist, since the former prevents the SiC growth while the latter is likely to enhance it. Such a compromise effect is also expected for varying the oxygen content, though the related materials were not available to be investigated.

3.4.4 Role of the polymer architecture

In addition to differences in the mere chemical composition of the system, differences in the architecture of the polymeric precursor within the same chemical system may be important. Both polycarbovinylsilazane (PVSZ)[7,9,12] and polycarbosilazane (PCSZ)[3,15] polymers were used as precursors for Si–C–N ceramics. They were not often compared until now in this paper because of the discrepancies in their heat-treatment conditions. However, comparisons remain reliable on some aspects. For instance, a main difference is the presence of vinyl groups in PVSZ instead of methyl groups in PCSZ. The existence of such primary C–C bonds may have a dramatic effect on the subsequent ceramic, regarding the carbon content. Actually, the carbon yield in the PVSZ-ceramic — calculated from the C/Si at. ratios in the polymer and the ceramic, respectively 2 and 1·6 — is higher (~ 82%) than in the PCSZ-based ceramics (60–70%, depending on the x value) — where C/Si at. ratios for the polymer and the ceramic are 1·6 and 1·08 respectively for the highest (for $x = 0{\cdot}25$). As a matter of fact, TEM investigations account for a much higher free-carbon content in the former material.[12,13] Though NMR investigations have shown[24] that the primary π C=C bonds transform into σ C–C bonds during the organic/inorganic transition (which occurs at low temperature, i.e. mainly below 500°C), a PVSZ precursor is thus more likely to finally promote a well and early developed polyaromatic carbon network, inducing dramatic consequences on the SiC nucleation then growth, as described in Section 3.3.4. Obviously, the fact that carbon atoms are neighboring in the starting polymer thus helps to promote the formation of aromatic rings as soon as the temperature of carbonisation is reached (>500°C) during the ceramisation step.

3.5 Influence of extrinsic parameters (i.e. related to the treatment conditions)

Using a gaseous N_2 atmosphere instead of an argon atmosphere during the heat-treatment of nitrogen-containing ceramics delays the SiC growth by maintaining the N content longer is the intergranular phase.[12,17,20] This indicates that gaseous N_2 is a by-product of the thermal evolution in the related chemical systems, and that nitrogen-containing intergranular phases such as SiC_xN_y may somewhat behave as Si_3N_4 relative to the free-carbon phase:

$$Si_3N_4(s) + 3\ C(s) \rightarrow 3\ SiC(s) + 2\ N_2(g) \quad (7)$$

which provides a vague idea of how the SiC_xN_y phase degrades. Maintaining the N atoms within the system long enough, regarding the temperature,

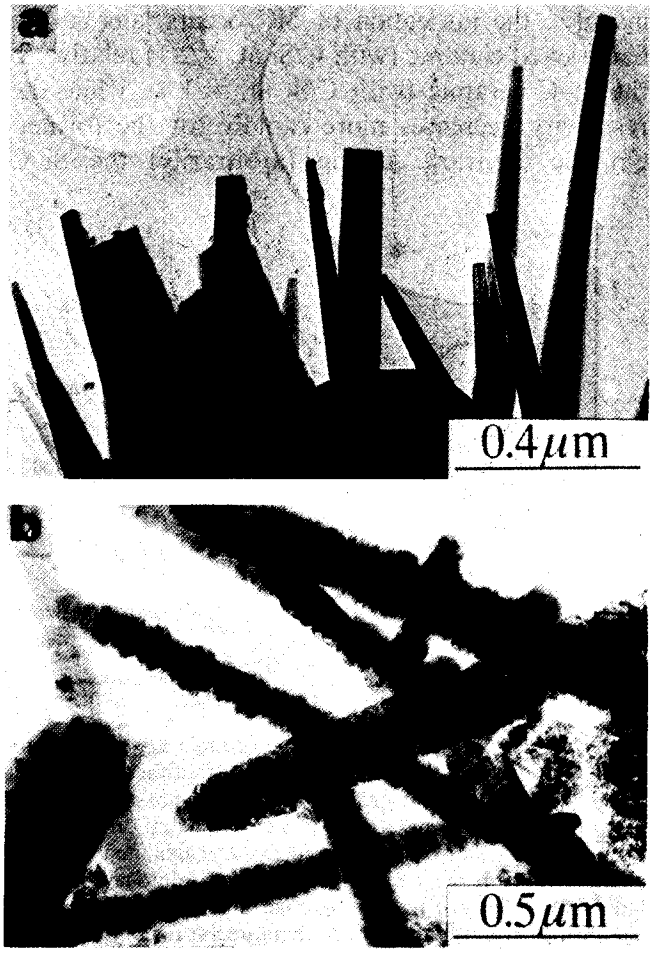

Fig. 15. BF images of (a) Si_3N_4 whiskers upon a Si–C–N–O ceramic surface[20] and (b) SiC whiskers grown upon the surface a PCSZ-based Si–C–N ceramic ($x = 0{\cdot}5$).[13]

might also of course lead to the formation of β-Si_3N_4 crystals in the bulk.[12] However, specific conditions may be required, such as a limited previous SiC crystallisation in order to maintain sufficient amounts of available Si atoms. The conditions were fullfilled in the PVSZ-based Si–C–N ceramics only,[12] though it is not ascertain whether they are due to the use of non-standard pyrolysis conditions (50°C/h instead of 3600°C/h) or to the specificity of the polymeric precursor (see Sections 3.4.4 and 3.3.4). Whatever, further studies should be made in order to investigate the extent of the reaction

$$3\ SiC(s) + 2\ N_2(g) \rightarrow Si_3N_4(s) + 3\ C(s) \quad (8)$$

in these chemical systems.

In contrast, a N_2 atmosphere and high temperatures (~ 1600°C) may promote α-Si_3N_4 whisker growth at the ceramic surface following reactions (5) and (6) for instance,[17,20] supporting the statement made in Section 3.3.4 that the partial pressure of self-induced released gaseous N_2 was not sufficient to allow these reactions to occur in argon atmosphere (Fig. 15(a)).

SiC-whiskers were also observed at high temperature (under argon atmosphere) at the surface of the PCSZ-based Si–C–N ceramic[13,15] (Fig. 15(b)). Likewise, this indicates that at least one of the gaseous species required was absent — or not in sufficient amount — in the inner atmosphere (i.e. filling the material porosity) but present in the surrounding atmosphere. O_2 traces are suspected (leaks, impurities in argon), able to promote the SiC whisker growth through reactions (1) and (2) from the gaseous Si species exiting the material. Previous reactions such as

$$C(s) + O_2(g) \rightarrow CO_2(g) \quad (9)$$

$$C(s) + CO_2(g) \rightarrow 2\ CO(g) \quad (10)$$

$$C(s) + 1/2\ O_2(g) \rightarrow CO(g) \quad (11)$$

$$Si(g) + 1/2\ O_2(g) \rightarrow SiO(g) \quad (12)$$

may have to occur depending upon the partial pressure of the species and the temperature in order to provide the oxygenated gaseous species required. In reactions (9) – (11), the C(s) species is provided by the graphite-body of the furnace. Indeed, previous studies on related materials have shown that environmental carbon added to oxygen traces may lead to unexpected events.[35] The fact that no SiC whiskers are formed for Si–C ceramics is explained by the lack of Si species exiting the material, since quite thermally stable (see Fig. 6).

Attention has to be paid that, as far as bond-breaking at high temperatures is involved, specifically when nitrogen-containing intergranular phases thermally degrade, radicals and radical reactions may also intervene in the whisker formation instead of or in addition to the regular gaseous species and chemical reactions listed above.

Finally, changing the heating rate also appears not to be subordinate. Because of the low porosity size, diffusion rates of gaseous species are low. Then, partial pressures of the gaseous species released by the materials are as higher as the heating rate is higher, i.e. the system acts as a more and more confined one. Therefore, as soon as any inner event is diffusion-controlled because involving a gaseous species (e.g. intergranular phase degradation and subsequent SiC growth in heteroatom-containing ceramics, or intrinsic Si_3N_4 crystallisation in PVSZ-based Si–C–N ceramic in N_2 atmosphere), its occurrence will be delayed and possibly inhibited by the use of high heating rate.[12]

4 Conclusion

The long-term investigation of polymer-based ceramics from the Si–C–N–O system which is reported and summarized in this paper has allowed the respective role and behavior of excess C, O, or N atoms to be revealed. An overall conclusion of the study could be that heteroatoms (regarding the SiC phase) should be avoided since finally always detrimental to the ceramic material at high temperatures. On the contrary, excess carbon may be considered beneficial to the stability of the ceramic material since limiting the SiC nucleation and SiC growth extent, and also beneficial to the mechanical properties since adding its own qualities to the properties of the bulk provided that the carbon amount is high enough to make the formation of an interconnected carbon network possible. As a matter of fact, recent development and investigations of heteroatom-free (or poor) fibers[32–34,36–46] exhibiting high thermal stability seems to sustain the idea that the binary Si–C chemical system is the more suitable for high temperature reinforcement applications. In some extent, it is true. However, although quite chemically stable, Si–C ceramics are found not to be as stable from a structural standpoint. Structural rearrangements occur continuously within the material, which could lead to fatal internal stresses when incorporated as a reinforcement within a brittle matrix such as SiC from chemical vapor deposition. In contrast, Si–C–N ceramics, although condemned to degrade at high temperatures, has been found to be thermochemically more stable than oxygen-containing systems, and more structurally stable than the Si–C system, at least within the stability domain. Therefore, Si–C–N fibers (prepared through an oxygen-free curing process)[18,47] may exhibit a stability domain wide enough to have a suitable potential as reinforcement for high temperature composites for uses below ~1400 - 1500°C, definitely better than oxygen-cured fibers, and possibly better than Si–C fibers. Furthermore, using nitrogen-containing polymers may help in limiting the extent of the carbon network in addition to inhibiting the structural rearrangements into SiC_4 tetrahedra. Actually, although demonstrated to be beneficial to the ceramic materials on the one hand, a well-developed long-range interconnected carbon network may be fatal for a use in oxygen-containing atmospheres on the other hand. Whatever, carbon is found to be the leading element in the SiC-based ceramics, since acting directly on the thermochemical and structural stabilities, the mechanical properties, the electrical behavior, and possibly the weavability of fibers. Further investigations of ceramics with various carbon content should therefore be necessary, and are actually currently performed in our laboratory.

Acknowledgements

The authors thank the National Program 'Précurseurs de Céramiques à Base Si, C, N, O' for its financial support and specifically the Centre National de la Recherche Scientifique (CNRS), the French Ministry of Defence (DRET), Rhône-Poulenc, and Société Européenne de Propulsion.

References

1. Pillot, J. P., Bacqué, E., Dunoguès, J. & Olry, P., Copolymérisation de dichlorosilanes avec des bischlorosilylmethanes, les produits obtenus et les utilisations desdits produits, *French Patent*, 2 599371, 1986.
2. Birot, M., Bacqué, E., Pillot, J.-P. & Dunoguès J., Etude de la transformation polydimethylsilane-polycarbosilane. I. Analyse des gaz dégagés. *J. Organomet. Chem.*, **310** (1986) C41–4.
3. Bacqué, E., Dunoguès, J., Biran, C., Olry, P. & Pillot, J.-P., *French Patent*, 2 599037, 1986.
4. Bacqué, E., Pillot, J.-P., Dunogués, J. & Olry, P., *European Patent*, 296028, 1988.
5. Monthioux, M., Oberlin, A. & Bouillon, E., Relations between microtexture and electrical properties during heat-treatment of SiC fiber precursor. *Compos. Sci. Technol.*, **37** (1990) 21–35.
6. Delverdier, O., Monthioux, M. & Oberlin, A., Rôle de l'oxygène dans l'evolution thermique de céramiques issues de polycarbosilane. In *Proceedings 7èmes Journées Nationales sur les Composites*, eds G. Fantozzi & P. Fleischmann. Lyon, France, 1990, pp. 391–400.
7. Lavedrine, A., Bahloul, D., Goursat, P., Choong, K. Y. N., Corriu, R., Leclercq, D., Mutin, H. & Vioux, A., Pyrolysis of polyvinylsilazane precursors to silicon carbonitride. *J. Europ. Ceram. Soc.*, **8** (1991) 221–7.
8. Richard, C., Bacqué, E., Pillot, J.-P., Birot, M., Dunoguès J., Mocaer, D. & Pailler R., In *Actes Journées Spéciales Fibres Minérales*. Paris, France, 1991, pp. 7–16.
9. Choong, K. Y. N., Corriu, R., Leclercq, D., Mutin, P. H. & Vioux, A., Polyvinylsilazane: a new precursor to silicon carbonitride. *New. J. Chem.*, **15** (1991) 85.
10. Bouillon, E., Langlais, F., Pailler, R., Naslain, R., Cruège, F., Huong, P. V., Sartrou, J. C., Delpuech, A., Laffon, C., Lagarde, P., Monthioux, M. & Oberlin, A., Conversion mechanisms of a polycarbosilane precursor into a SiC-based ceramic material. *J. Mater. Sci.*, **26** (1991) 1333–45.
11. Bouillon, E., Mocaer, D., Villeneuve, J.-F., Pailler, R., Naslain, R., Monthioux, M., Oberlin, A., Guimon, C. & Pfister, G., Composition-microstructure-property relationships in ceramic monofilaments resulting from the pyrolysis of a polycarbosilane precursor at 800 to 1400°C. *J. Mater. Sci.*, **26** (1991)1517–30.
12. Delverdier, O., Monthioux, M., Oberlin, A., Lavedrine A., Bahloul, D. & Goursat, P., Thermal behaviour of polymer-derived ceramics. II. Si–C–N system from a new PVSZ precursor. *J. High Temp. Chem. Process.*, **1** (1992) 139–49.
13. Delverdier, O., Monthioux, M., Mocaer, D. & Pailler, R., Thermal behaviour of polymer-derived ceramics. III. Si–C–N system from a new PCSZ precursor. In *5th European Conference on Composite Materials Proceedings*, eds A. R. Bunsell, J. F. Jamet & A. Massiah. Bordeaux, France, 1992, pp. 691–6.
14. Pailler, R., Jaymes, I., Naslain, R., Richard, C., Pillot, J. P., Dunoguès, J., Olry, P., Mocaer, D. & Chassagneux, E., Effects of oxygen content on mechanical properties and oxidation resistance in ex-PCSZ Si–C–N–O model filaments. In *5th European Conference on Composite Materials Proceedings*, eds A. R. Bunsell, J. F. Jamet & A. Massiah. Bordeaux, France, 1992, pp. 631–6.
15. Mocaer, D., Pailler, R., Naslain, R., Richard, C., Pillot, J.-P., Dunoguès, J., Gérardin, C. & Taulelle, F., Si–C–N ceramics with a high microstructural stability elaborated from the pyrolysis of new polycarbosilazane precursors. Part I. The organic-inorganic transition. *J. Mater. Sci.*, **28** (1993) 2615–31.
16. Mocaer, D., Pailler, R., Naslain, R., Richard, C., Pillot, J.-P. & Dunoguès, J., Si–C–N ceramics with a high microstructural stability elaborated from the pyrolysis of new polycarbosilazane precursors. Part II. Effect of oxygen curing on properties of ex-PCS monofilaments. *J. Mater. Sci.*, **28** (1993) 2632–8.
17. Mocaer, D., Pailler, R., Naslain, R., Richard, C., Pillot, J.-P., Dunoguès, J., Delverdier, O. & Monthioux, M., Si–C–N ceramics with a high microstructural stability elaborated from the pyrolysis of new polycarbosilazane precursors. Part III. Effect of pyrolysis conditions on the nature and properties of oxygen-cured derived monofilaments. *J. Mater. Sci.*, **28** (1993) 2639–53.
18. Mocaer, D., Pailler, R., Naslain, R., Richard, C., Pillot, J.-P., Dunoguès, J., Darnez, C., Chambon, M. & Lahaye, M., Si–C–N ceramics with a high microstructural stability elaborated from the pyrolysis of new polycarbosilazane precursors. Part IV. Oxygen-free model monofilaments *J. Mater. Sci.*, **28** (1993) 3049–58.
19. Delverdier, O., Monthioux, M., Mocaer, D. & Pailler, R., Thermal behavior of polymer-derived ceramics. I. Si–C and Si–C–O systems from both commercial and new polycarbosilane (PCS) precursors. *J. Europ. Ceram. Soc.*, **12** (1993) 27–41.
20. Delverdier, O., Monthioux, M., Mocaer, D. & Pailler, R., Thermal behavior of polymer-derived ceramics. IV. Si–C–N–O fibers from an oxygen-cured polycarbosilazane. *J. Europ. Ceram. Soc.*, **14** (1994) 313–25.
21. Le Coustumer, P., Monthioux, M. & Oberlin, A., Understanding Nicalon^R fiber. *J. Europ. Ceram. Soc.*, **11** (1993) 95–103.
22. Bourgerette, C., Le Coustumer, P., Monthioux, M. & Vahlas, C., TEM characterization of a heat treated

Tyranno^R fiber. In *6th European Conference on Composite Materials. Proceedings, vol: High temperature ceramic matrix composites,* eds. R. Naslain, J. Lamon & D. Doumeingts, Woodhead Publishing Limited, UK. Bordeaux, France, 1993, pp.67–74.

23. Oberlin, A., Carbonization and graphitization. *Carbon,* **22** (1984) 521–41.
24. Gérardin, C., Caractérisation par résonance magnétique nucléaire de matériaux céramiques à base de carbure ou carbonitrure de silicium obtenus par voie polymérique. PhD Thesis, University of Paris VI, France, 1991.
25. Oberlin, A., Boulmier, J.-L. & Villey, M., Electron microscopy study of kerogen microtexture Selected criteria for determining the evolution stage of kerogen. In *Kerogen,* ed. B. Durand, Technip, Paris, France, 1980, pp.191–241.
26. Goma, J., Oberlin, A., Kerrand, E. & Bélouet, C., Résistance du substrat de carbone au silicium fondu dans le procédé RAD. *Rev. Phys. Appl.,* **19** (1984) 297–306.
27. Greil, P., Thermodynamic calculations of Si–C–O fiber stability in ceramic matrix composites. *J. Europ. Ceram. Soc.,* **6** (1990) 53–64.
28. Vorpagel, R. E. & Lavin, J. G., Most stable configurations of polynuclear aromatic hydrocarbon molecules in pitches via molecular modelling. *Carbon,* **30** (1992) 1033–40.
29. Le Coustumer, P., Monthioux, M. & Oberlin, A., Mécanismes de dégradation d'une fibre Nicalon série 200. In *AMAC-CODEMAC Colloquium: Matériaux Réfractaires pour Applications Hautes Températures,* eds. R. Naslain, J. Lamalle & J. L. Zulian. Bordeaux, France, 1990, pp. 43–53.
30. Schamm, S., Mazel, A., Dorignac, D. & Sevely, J., HREM identification of 'one dimensionally disordered' polytypes in the SiC (CVI) matrix of SiC/SiC composites. *Microsc. Microanal. Microstruct.,* **2** (1991) 59–73.
31. Madigou, V., Monthioux, M. & Oberlin, A., Microstructure et microtexture d'un composite Si_3N_4 renforcé whiskers et de ses constituants. In *AMAC-CODEMAC Colloquium: Matériaux Réfractaires pour Applications Hautes Températures,* eds R. Naslain, J. Lamalle & J. L. Zulian. Bordeaux, France, 1990, pp. 221–35.
32. Chollon, G., Laporte, C., Pailler, R. Naslain, R. Laanani, F., Monthioux, M. & Olry P., Thermal stability of a PCS-derived fiber with a low oxygen content (Hi-Nicalon). *J Mater. Sci.* (submitted).
33. Chollon, G., Fibres céramiques à base de carbure de silicium et à faible taux d'oxygène. PhD Thesis, University of Bordeaux I, France, 1995.
34. Laanani, F., Monthioux, M., Guimon, C., Chollon, G. & Pailler, R., A comparative study of some heat-treated oxygen-cured or radiation-cured ceramic fibers: chemical, structural, and nanotextural aspects. *J. Europ. Ceram. Soc.* (to be submitted).
35. Le Coustumer, P., Monthioux, M. & Oberlin, A., Further studies of the stability of PCS-based ceramic fibres at high temperatures. 2. Effect of all-carbon environments. *Br. Ceram. Trans. J.,* **94** (1996) 185–90.
36. Matsuzawa, T., Okamura, K. & Sato, M., Microstructure and mechanical properties of SiC fiber. In *International Meeting on Advanced Materials,* Vol. 4, Materials Research Society, 1989, pp.191–6.
37. Okamura, K., Sato, M., Seguchi, T. & Kawanishi, S., Preparation of high temperature strength SiC fiber. In *Controlled Interphases in Composites Materials,* ed. H. Ishida, Elsevier, 1990, pp. 209–18.
38. Takeda, M., Imai, Y., Ichikawa, H., Ishikawa, T., Seguchi, T. & Okamura, K., Properties of the low oxygen content SiC fiber on high temperature heat-treatment. *Ceram. Eng. Sci. Proc.,* **12** (1991) 1007–18.
39. Yamamura, T., Tyranno fibers. In *Euro-Japanese Colloquim on Ceramic Fibers, 6th European Conference on Composites Materials,* eds A. R. Bunsell & I. Kimpara, Bordeaux France, Japan Society for Composites Materials, 1993, pp. 187–201.
40. Xu, Y., Zangvil, A., Lipowitz, J., Rabe, J. A. & Zank, G. A., Microstructure and microchemistry of polymer-derived crys-talline SiC fibers, *J. Am. Ceram. Soc.,* **76** (1993) 3034–40.
41. Ishikawa, T., Recent developments of the SiC fiber Nicalon and its composites, including properties of the SiC fiber Hi-Nicalon for ultra-high temperature. *Compos. Sci. Technol.,* **51** (1994) 135–44.
42. Toreki, W., Batich, C. D., Sacks, M. D., Saleem, M., Guang, J. C. & Morrone, A. A., Polymer-derived silicon carbide fibers with low oxygen content and improved thermomechanical stability. *Compos. Sci. Technol.,* **51** (1994) 145–59.
43. Hasegawa, Y., New curing method for polycarbosilane with unsaturated hydrocarbons and application to thermally stable SiC fibre. *Compos. Sci. Technol.,* **51** (1994) 161–6.
44. Lipowitz, J., Barnard, T., Bujalski, D., Rabe, J & Zank, G., Fine-diameter polycristalline SiC fibers. *Compos. Sci. Technol.,* **51** (1994) 167–71.
45. Takeda, M., Sakamoto, J., Imai, Y., Ichikawa, H. & Ishikawa, T., Properties of stoichiometric silicon carbide fiber derived from polycarbosilane. *Ceram. Eng. Sci. Proc.,* **15** (1994) 133–41.
46. Zhang, Z.-F., Scott, C. S. & Laine, R. M., Pure silicon carbide fibers from polymethylsilane. *Ceram. Eng. Sci. Proc.,* **15** (1994) 152–61.
47. Sato, M. Okamura, K., Kawanishi, S. & Seguchi, T., Preparation and mechanical properties of silicon oxynitride fiber and silicon nitride fiber. In *International Meeting on Advanced Materials,* Vol. 4, Materials Research Society, 1989, pp. 197–202.